Photochemistry and Photobiology, Vol. 62, No. 2, pp. 279–289, 1995
Printed in the United States. All rights reserved

0031-8655/95 $05.00+0.00

CHLOROPHYLLS IN POLYMERS. I. STATE OF CHLOROPHYLL *a* IN UNSTRETCHED POLYMER SYSTEMS

M. A. M. J. VAN ZANDVOORT*, D. WRÓBEL†, P. LETTINGA, G. VAN GINKEL and Y. K. LEVINE
Debye Institute, Buys Ballot Laboratory, Princetonplein 5, 3584 CC Utrecht, the Netherlands

(*Received* 25 *August* 1994; *accepted* 22 *March* 1995)

Abstract—Model systems for the study of energy transfer processes are useful for the elucidation of the various factors governing the mechanism of energy transfer in photosynthetic systems. Here we describe the characterization of two systems, consisting of chlorophyll *a* incorporated in anhydrous nitrocellulose and polyvinylalcohol films. First, optical spectroscopy and time-resolved fluorescence techniques are used to characterize the state of the chlorophyll molecules in the films. We find that in nitrocellulose films the state of chlorophyll *a* depends strongly on the ratio of nitrocellulose to dimethylsulfoxide in the solutions from which the films are cast. The state of chlorophyll *a* in polyvinylalcohol films does not depend on the amount of polymer originally dissolved in dimethylsulfoxide. In these films the pigment is monomeric at low concentrations of chlorophyll *a*, but aggregates are formed at much lower concentrations than in nitrocellulose. The latter fact is explained by the existence of pockets in polyvinylalcohol, leading to high local concentrations.

To further test the suitability of the nitrocellulose polymer films as model systems for energy transfer processes, time-resolved fluorescence anisotropy profiles are measured in dependence of the concentration of pigments in the matrix. Fits of the observed decay profiles to the predicted decay show good correspondence, as long as no traps are present. Furthermore, the fitted decay times yield the correct value of the Förster radius R_0 as compared to the value obtained spectroscopically. We thus conclude that the chlorophyll *a*–nitrocellulose system can be very appropriate for the study of energy transfer processes between photosynthetic pigment, since the pigments are uniformally distributed in the matrix.

INTRODUCTION

Chlorophyll *a* (Chl *a*)‡ is the main pigment in the photosynthetic process,[1] which takes place in green plants and most algae. In the photosynthetic process solar energy is converted into chemical energy. The light-harvesting step in photosynthesis depends on a highly efficient interpigment energy transfer (ET) process. Also in *in vitro* systems chlorophyll molecules exhibit ET.[2–8] Therefore, in order to elucidate the role of the different factors governing ET in the light-harvesting step, much research effort has been directed toward the preparation of stable systems in which these factors can be studied. To this end, the Chl *a* molecules were embedded in a wide variety of matrices (such as apolar solvents, lipid bilayers, nematic liquid crystals and Langmuir–Blodgett films). By comparison, relatively little attention was paid to the use of polymers[9–12] as a host system for Chl *a*. These latter hosts offer several major advantages over the former systems. The pigments are immobilized within the polymer matrix at room temperature, so that the orientation factor of the Förster theory for ET[13] is time independent. The pigments can also be aligned macroscopically to a high degree by stretching the films.[14–24] Finally, the distances between the pigments can be varied by changing their concentration in the polymer matrix provided no aggregates are formed. The basic assumption underlying the usefulness of polymer films for ET studies is that the pigment molecules are uniformly distributed in the matrix.

Here we report a study of the characterization of two model systems consisting of Chl *a* in anhydrous polyvinylalcohol (PVA) and nitrocellulose (NC) polymers. The results build on our previous investigation[25] of the spectral and physical properties of Chl *a* embedded in anhydrous PVA films cast from dimethylsulfoxide (DMSO) at concentrations below 5×10^{-7} mol/g. It was shown that in these films the Chl *a* is present in a monomeric form only. The efficient ET and excitation trapping observed was ascribed to the organization of the Chl *a* molecules in pocket-like structures. Here we focus on the state of Chl *a* in PVA films at higher concentrations and we conclude that the Chl *a*/PVA system is only useful for the study of the ET processes in the presence of a large concentration of traps.

Also the Chl *a*/NC films were cast from solutions in DMSO. We have found that the ratio of NC to DMSO in the solutions used determines the state of the Chl *a* in the films. Films cast from a solution containing higher NC/DMSO ratios always contain NC–Chl *a* complexes. On the other hand, a monomeric state is found in films cast from solutions containing less than 0.5 g NC per 5 mL DMSO. The Chl *a* concentration in these films can be varied over a broad range covering the entire region from noninteracting molecules to the formation of traps.

*To whom correspondence should be addressed.
†Present address: Institute of Physics, Poznań Technical University, Piotrowo 3, 60-965-Poznań, Poland.
‡*Abbreviations:* Chl *a*, chlorophyll *a*; DMSO, dimethylsulfoxide; ET, energy transfer; FWHM, full width at half maximum; GAF, Gochanour, Andersen and Fayer; HBB, Huber, Hamilton and Barnett; NC, nitrocellulose; PVA, polyvinylalcohol.

The question arises now as to whether the molecules in the latter type of films are in fact uniformly distributed throughout the NC matrix. In particular it is important to establish that the distances between the pigments scale with concentration and that in unstretched NC films their mutual orientations are randomly distributed. The distribution of the pigments is most conveniently studied by monitoring the effects of intermolecular ET processes on the fluorescence anisotropy decays. These decay curves obtained from films containing different pigment concentrations can be analyzed in terms of the generalized Master equation for the donor–donor ET migration, based on the Förster ET mechanism.[13,26–33] Now the anisotropy decay time is inversely proportional to the square of the reduced concentration defined as the average number of pigments contained in a sphere of the Förster radius R_0. For a uniform pigment distribution the reduced concentration is proportional to the average concentration.[30–33] Consequently, the anisotropy decay time will scale with average concentration. Moreover, the Förster radius R_0 can be determined from the concentration dependence of the anisotropy decay time. The value for R_0 extracted in this way should correspond to that calculated directly from the absorption and emission spectra of Chl *a* in the films.[30–34] Deviations from a uniform distribution will be manifested in discrepancies in the values of R_0 obtained with these two methods. These discrepancies reflect both microcorrelations in the mutual orientations and distances of the pigments.[30–33]

A short discussion of the theoretical approach to the analysis of fluorescence anisotropy decay in the presence of ET processes is first given. After the spectral characterization of the Chl *a*–PVA and Chl *a*–NC systems, this theory is then applied to the latter system for the extraction of the Förster radius of Chl *a* from the experimental decay curves. The results obtained are consistent with those expected for a uniform pigment distribution in the NC films. We thus conclude that the Chl *a*–NC system can be readily used for donor–donor ET studies, and in a following paper we will discuss the influence of stretching on these films.

THEORY OF ENERGY TRANSFER

The master equation for energy migration

When light is incident on an ensemble of identical fluorescent molecules one or more molecules will undergo a transition into the excited state. In the absence of intermolecular interactions, for instance at low concentrations, the excited molecules will relax to the ground state with the emission of a photon. The average residence time of the molecules in the ensemble in the excited state is called the fluorescence lifetime τ. In the presence of intermolecular interactions, which can be modulated by the local molecular concentration, an excited pigment can transfer its excitation energy to a neighboring pigment and energy migration over the ensemble takes place. When the interactions are very weak, for instance because the distances between molecules are large compared to their dimension, the excitation is localized on one of the pigments in the ensemble at all times. If furthermore, the new excited state undergoes a fast dephasing due to vibrational interactions, the ET process is incoherent.[26,27,35] Now the probability $P_i(t)$ of finding pigment i in an excited state at time t can be described by coupled rate equations known as the master equation of energy migration.[28]:

$$\frac{d}{dt}P_i = -\frac{P_i}{\tau} + \sum_k (w_{ki}P_k - w_{ik}P_i). \qquad (1)$$

List of Symbols

κ^2	Factor describing the mutual orientation of the emission moment of the excited molecule and the absorption moment of the accepting pigment.
λ	Wavelength in nm.
$\hat{\mu}_k$	The absorption transition dipole moment.
$\hat{\nu}_i$	The emission transition dipole moment.
ρ	The average pigment concentration in the sample.
$\hat{\rho}$	The reduced pigment concentration, being the average number of molecules within a sphere with a radius R_0.
τ	The fluorescence lifetime of a pigment.
τ_0	The natural lifetime of a pigment.
$\epsilon(\lambda)$	The spectrum of the extinction coefficient against the wavelength.
$F(\lambda)$	The unnormalized fluorescence spectrum.
g_{stat}	Orientational averaging factor of a pigment ensemble.
n	Refractive index of the medium in which the pigments are embedded.
N(t)	The total fluorescence decay.
$N_0(t)$	The probability that a molecule excited at t = 0 is still excited at t = t.
$P_i(t)$	The probability of finding pigment i in an excited state at time t.
Q_Y	The red absorption band of monomeric chlorophylls.
$\hat{r}$	The unit vector connecting the centers of mass of the two interacting pigments.
R_0	The Forster distance.
R_{ik}	The distance between the centers of mass of two interacting pigments.
S	The Sorbet absorption band.
w_{ik}	The rate of excitation transfer from molecule i to molecule k.

Here the first term describes the fluorescence decay of the individual pigments. The second term accounts for the decay arising from the ET. The factors w_{ik} denote the rate of excitation transfer from molecule i to molecule k. Within the framework of Förster theory (valid if the pigments are separated by distances larger than their dimensions[36]), only dipole–dipole interactions are considered and the transfer rates are given by [30–33]

$$w_{ik} = \frac{3}{2}\kappa^2 \frac{1}{\tau_0}\left(\frac{R_0}{R_{ik}}\right)^6. \qquad (2)$$

In this expression τ_0 is the natural lifetime of the pigment, which is longer than the experimentally observed radiative lifetime τ. The ratio τ/τ_0 denotes the fluorescence quantum yield. The term R_0 is the Förster radius defined as the dis-

tance between two molecules for which the probabilities of ET and fluorescence emission are equal. Then, R_{ik} is the distance between the centers of mass of the two interacting molecules. Finally, κ^2 is the factor describing the mutual orientation of the emission moment $\hat{\nu}_i$ of the excited molecule and the absorption moment $\hat{\mu}_k$ of the accepting pigment and is given by [30–33]

$$\kappa^2 = [(\hat{\mu}_k\hat{\nu}_i) - 3\,(\hat{\mu}_k\hat{r}_{ik})(\hat{\nu}_i\hat{r}_{ik})]^2 \qquad (3)$$

where $\hat{r}$ is the unit vector connecting the centers of mass of the two interacting pigments. We note that the transfer rates for isotropic systems containing immobilized pigments are obtained simply on averaging κ^2 over an isotropic orientational distribution.[30–33]

The natural lifetime can be calculated directly from the measured absorption, $\epsilon(\lambda)$, and emission, $F(\lambda)$, spectra of the monomeric pigments embedded in a medium of refractive index n[37]:

$$\frac{1}{\tau_0} = 2.88 \times 10^{-9} n^2 \frac{\int F(\lambda)\lambda^{-2}\,d\lambda}{\int F(\lambda)\lambda\,d\lambda} \int \epsilon(\lambda)\lambda^{-1}\,d\lambda \quad [s^{-1}]. \qquad (4)$$

The master equation is conventionally solved using the initial condition $P_i(0) = \delta_{ik}$.[30–33]

The solution of the master equation for immobilized, isotropically distributed pigments

The solutions of the coupled rate equations (Eq. 1) are approximated within the Gochanour, Andersen and Fayer (GAF) formalism by a method previously described[30–33] and will only be summarized here. This approach utilizes a diagrammatic series expansion of the Green function solution to the coupled rate equations for the occupation probabilities $P_i(t)$ of individual donors. The part of the Green function describing the probability $N_0(t)$ that a molecule excited at time $t = 0$ is still excited at time t later is shown to be given accurately by the so-called three body approximation, which only takes into account interactions between three pigments. The results of this three body model are also well reproduced by more heuristic approaches.[30–33,38] Of these, the Huber, Hamilton and Barnett (HBB) model with a back-transfer correction is especially appealing and will be used here for the sake of simplicity.[30–33,39] In the limit of a three-dimensional system of immobilized and isotropically distributed pigments this latter model yields[29–33]

$$\log N_0(t) = -\frac{t}{\tau} - 2^{-1/2} g_{stat} \sqrt{\pi} \sqrt{\hat{\rho}^2 \frac{t}{\tau_0}}. \qquad (5)$$

Here, g_{stat} is a factor arising from the orientational averaging of κ^2 over the pigment ensemble and is for immobilized, isotropically distributed pigments[30–33] equal to 0.8452. Furthermore, $\hat{\rho}$ is the reduced concentration, being the average number of molecules in a sphere with radius R_0. For a uniform distribution of pigments in the medium it is simply connected to the average pigment concentration ρ as[30–33]

$$\hat{\rho} = \frac{4}{3}\pi R_0^3 \rho. \qquad (6)$$

It can be seen from Eq. 5 that in the presence of ET processes the monoexponential decay of N_0 due to radiative emission is modulated by an additional exponential decay process whose time course varies with $\sqrt{t}$ and whose time constant is directly related to the reduced concentration.

It is now important to realize that the averaging procedure involved in the calculation of g_{stat} needs to be modified in the presence of microcorrelations between the pigment molecules.[30–33] While this does not by itself modify the time dependence of $N_0(t)$, it will compromise the relation between the average and reduced concentrations. Consequently, the application of Eq. 5 and 6 will yield distorted values for the Förster radius R_0.

The observable in ET studies

In the so-called Galanin approximation[40] ET processes are considered to fully depolarize the electronic excitations. Consequently polarized fluorescence emission will only be observed from those pigment molecules that were initially excited. This approximation is generally considered to be valid for systems containing randomly oriented pigment molecules in the absence of microcorrelations. It has been shown[30–33] that under these conditions r(t) is related to $N_0(t)$ as:

$$r(t) = r(0)\frac{N_0(t)}{N(t)} \qquad (7)$$

where N(t) is the total fluorescence decay ($e^{-t/\tau}$, the intrinsic fluorescence decay, for a pure donor system) and $r(0) = 0.2(3\cos^2\epsilon - 1)$ with ϵ the angle between the absorption and emission transition dipole moments.

Spectral determination of the Förster radius

The Förster radius R_0 can be determined experimentally from the absorption and emission spectrum of a pigment embedded in a medium of refractive index n[13]:

$$R_0^6 = 8.79 \times 10^{-25} \frac{\langle\kappa^2\rangle}{n^4} \frac{\int F(\lambda)\epsilon(\lambda)\lambda^2\,d\lambda}{\int F(\lambda)\lambda^{-2}\,d\lambda} [cm^6]. \qquad (8)$$

Conventionally $\langle\kappa^2\rangle$ is taken to be equal to ⅔ to conform with the original derivation of the Förster theory in the limit of fast reorientational motions.[13] In fact, the incorporation of this value in R_0 results in the factor ½ in Eq. 2. We note that the determination of R_0 in this way requires the spectra to be corrected for instrument response.

The independent determination of R_0 from photophysical data serves as a check on the values extracted for this parameter from an analysis of the fluorescence anisotropy decay curves. Systematic discrepancies are taken to be indicative of a breakdown of the assumptions of uniform, isotropic pigment distribution in the polymer matrix.

MATERIALS AND METHODS

Sample preparation. Chlorophyll *a* was extracted from fresh spinach leaves (either obtained from the local market or cultivated in the laboratory) according to the method of Terpstra and Lambers[41]

and purified using thin-layer chromatography. A stock solution of Chl *a* in acetone was stored at −25°C. The purity of this solution over a period of weeks was checked using isocratic reversed-phase HPLC.[42] In this way we were able to rule out the presence of optically indistinguishable Chl *a* derivatives, such as Chl *a'*[43-50] and allomerized Chl *a*.

Acetone and DMSO of analytical grade purity were purchased from E. Merck and from J. T. Baker Chemicals B. V., respectively, and used without further purification. One hundred percent hydrolyzed PVA with an average weight of about 100 kDa was obtained from Aldrich-Chemie and cleaned from side product (acidic traces and residual acetyl groups) by the modified ethanol extraction method described in van Zandvoort *et al.*[25] The NC powder was obtained from Wolff Walsroder A.G. and purified before use in the following way: NaOH with a final concentration of 0.01 *M* was added to NC powder and kept in the dark under continuous stirring for 20 h. The mixture was then cleaned several times with water and dried at room temperature under a continuous nitrogen stream. Using this method, acid traces and radicals in the NC powder were removed. The preparation of the Chl *a*–PVA solutions and of the dried PVA films has been described by us previously.[25] Chlorophyll *a*–NC solutions are prepared by mixing 5 mL DMSO with the desired amounts of dried Chl *a*. Then the NC powder is added, followed by stirring for 15 min at room temperature. The concentration of NC was varied in a range of 0.1–2 g per 5 mL DMSO. From these solutions films were obtained by the same evaporation procedure as used for PVA films. For the ET studies, only samples prepared from 0.3 g of NC in 5 mL DMSO were used.

Final concentrations of Chl *a* in solutions were in the range of 10^{-5}–10^{-7} *M*. Final concentrations of Chl *a* in films were in the range of 5×10^{-8} to 10^{-5} mol/g for NC and 10^{-7} to 5×10^{-6} mol/g for PVA.

The thickness of the film was chosen so that their optical densities were below 0.1 so as to avoid reabsorption effects. The dried films were placed between thin glass plates using ultrapure glycerol (n = 1.52) for ensuring optical contact. The samples were sealed round their edges and masked with black tape, leaving a spot of 2 mm in diameter for illumination. The refractive index of the NC films was measured with an Abbe refractometer and found to be 1.52 ± 0.01.

Experiments. The density of pure NC films cast from solutions of different NC/DMSO ratios was measured. The length and width of a rectangular piece of film were measured with a micrometer and its weight was determined with an analytical balance. This was necessary because the NC/DMSO ratio appears to influence the morphology of the polymer film.

Absorption spectra were measured with a DW2000 spectrophotometer (SLM-Aminco). The spectra of all the Chl *a* samples were corrected for the absorption of the polymer matrix. The value of the extinction coefficient, needed for the ET studies, was determined from the absorption spectra, making use of the density of NC films. The excitation and emission spectra were measured using an SPF 500 SLM-Aminco spectrofluorometer. An L-format geometry was used. The films were mounted in a special holder so that their surfaces made an angle of 45° with the incident and emitted beam. Excitation spectra were normalized to the highest peak and were measured using narrow-band emission (2 nm), while the emission spectra were recorded using narrow-band excitation (2 nm). Emission spectra were normalized and corrected for instrument response using the known sensitivity curve of the photomultiplier tube.

The time-resolved fluorescence intensity and anisotropy decay measurements were carried out at the Synchrotron Radiation Source, Daresbury Laboratory (UK) as described previously.[51] The polarization sensitivity correction factor G for the setup was determined using a dilute Chl *a* solution in acetone. In all the experiments interference and cut-off filters were used for selecting the emission wavelength and the suppression of stray light. The pulse profile was measured using either a Ludox suspension or a blank film. The data were collected using a standard single photon counting setup equipped with a Philips XP2020Q photomultiplier tube.

Analysis. The intensity decay curves were fitted to multiexponential functions with a reiterative deconvolution algorithm using a nonlinear least-squares Marquardt procedure (ZXSSQ) from the IMSL library.

The fluorescence anisotropy at low concentrations, in the absence of ET, is given by[52,53]

$$r(t) = r(0) \sum_{i=1}^{N} \alpha_i \exp(-t/\phi_i) \tag{9}$$

where ϕ_i and α_i are, respectively, the rotational correlation time and amplitude of the decay component i and r(0) is

$$r(0) = 0.2(3\cos^2\epsilon - 1). \tag{10}$$

Here ϵ denotes the angle between the absorption and emission dipole moment. This angle is, however, dependent on the excitation and emission wavelengths used. In the first, spectroscopic part of this paper, we will use the absence of an anisotropy decay at low concentrations to demonstrate that rotational motion of the monomeric Chl *a* molecules is quenched.

At higher concentrations, in the presence of intermolecular ET processes, the anisotropy decay, Eq. 1 needs to be modified to take into account a nonexponential decay behavior.[30-32] In the second part of the study, the anisotropy decay curves were fitted to $e^{-\sqrt{t/T_c}}$ making use of a reiterative deconvolution algorithm using a nonlinear least-squares Marquardt procedure.

RESULTS

Spectroscopy

General. The spectral measurements described below are used to characterize the state of Chl *a* pigments in the polymer matrix. Monomeric Chl *a* exhibits absorption in two main regions[25]: the Soret region, 360–440 nm and the Q_Y-band, 640–680 nm. The peak positions and widths as well as the ratio of absorption in the maximum of the Soret band and in the maximum of the Q_Y band (S/Q_Y) of the monomeric spectrum are well established.[25] The emission spectrum of Chl *a* monomers consists of a main band centered at 670 nm and a much weaker band with a maximum around 720–740 nm. Aggregation or degradation of Chl *a* results in changes in all these spectral parameters.[25]

The fluorescence intensity decay of monomeric Chl *a* is monoexponential with a lifetime of around 5 or 6.5 ns depending on the coordination state of the Mg center.[54,55] Donor–donor ET processes among Chl *a* pigments do not influence this behavior. In the presence of traps, however, the fluorescence decay becomes a complex function, which is not easily described in an analytical form.[33] Here we shall use the deviation from the monoexponential decay process to monitor trap formation and the presence of different fluorescent species with a distinct lifetime.

Chl a in PVA films. The absorption spectra of Chl *a* in PVA films are shown in Fig. 1 at three different concentrations: 3×10^{-7} mol/g (curve 1), 5×10^{-7} mol/g (curve 2) and 5×10^{-6} mol/g (curve 3). The corresponding spectral parameters are summarized in Table 1. The spectrum obtained at the lowest concentration is characteristic for all Chl *a* concentrations in the range 5×10^{-8} mol/g to 4×10^{-7} mol/g and corresponds to the monomeric spectrum of Chl *a*.[25] At higher Chl *a* concentrations an extra peak on the red side of the Q_Y-band appears, leading to an increase in S/Q_Y and the full width at half maximum (FWHM) of the Q_Y-band. As revealed by derivative absorption spectroscopy (results not shown), this peak is centered at 694–696 nm. The height of this peak increases with Chl *a* concentration. In order to establish whether this peak arises from the formation of a fluorescent species, we have measured the emission and excitation spectra of Chl *a* in PVA at different concen-

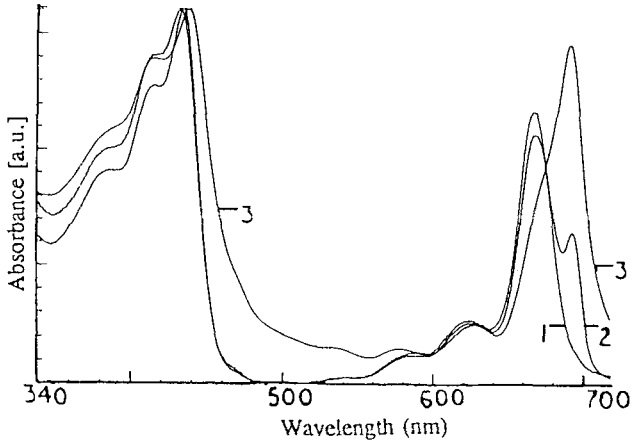

Figure 1. Absorption spectra of (1) Chl *a*/PVA film, concentration between 5×10^{-8} mol/g and 4×10^{-7} mol/g; (2) Chl *a*/PVA film, 5×10^{-7} mol/g; (3) Chl *a*/PVA film, 5×10^{-6} mol/g.

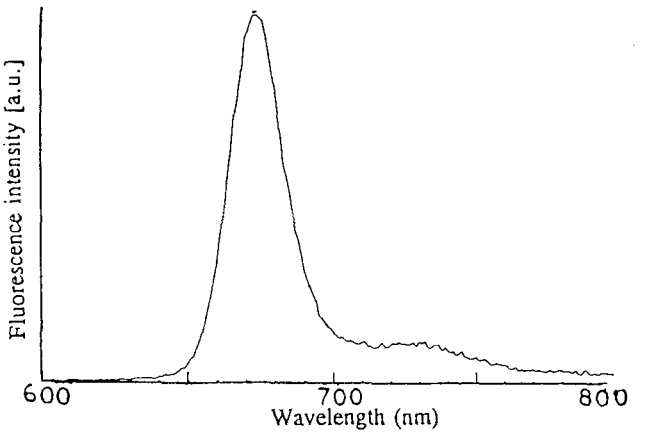

Figure 2. Emission spectra of Chl *a* in PVA films, NC–DMSO and NC films (low NC–DMSO ratio).

trations. Interestingly, we find that the emission spectrum is independent of both the excitation wavelength and concentration of Chl *a*, see Fig. 2 and Table 2. Furthermore, excitation in the new 694–696 nm band does not lead to any fluorescence intensity in the 696–800 nm region.

The excitation spectra of Chl *a*/PVA films over the whole concentration range are found to be independent of the emission wavelength and are identical to the monomeric absorption spectra. This shows that the absorption peak at 694–696 nm belongs to a nonfluorescent species. The fluorescence emission from the Chl *a*/PVA films thus arises wholly from monomeric Chl *a*.

These findings establish the formation of nonfluorescing Chl *a* aggregate in PVA films at concentrations above 4×10^{-7} mol/g. Consequently, these systems are considered to be useful models for studying ET in the presence of traps only below this Chl *a*/PVA concentration.

The fluorescence of pure NC in DMSO solutions and cast films. Knowledge of the fluorescence behavior of pure NC is a prerequisite in the study of the behavior of Chl *a* in NC films. To this end the absorption, excitation and emission spectra of pure NC–DMSO solutions and NC films were measured in the spectral range 340–800 nm. No significant difference was found between the spectral properties of NC in solution and in film (Fig. 3). These spectra show that NC only absorbs in the blue region (300–480 nm). The absorption spectra for the Chl *a*/NC systems presented below were corrected for the background absorption of NC. The NC absorption in the blue region gives rise to a broad and structureless fluorescence band at 510–540 nm. The fluorescence is much weaker than the Chl *a* fluorescence and therefore does not distort the Chl *a* fluorescence measurements.

Chl a in the NC–DMSO solutions. The absorption and emission spectra of Chl *a* in fresh NC–DMSO solutions are typical of monomeric Chl *a*[25] and their parameters are summarized in Tables 1 and 2, respectively. The spectra are moreover independent of the NC–DMSO ratio and the Chl *a* concentration used.

The fluorescence intensity decay of Chl *a* is found to be independent of the excitation and emission wavelength and is best described by a monoexponential function with a lifetime of 4.7 ns (Table 3). This is only slightly shorter than the 5 ns reported for monomeric Chl *a* in DMSO and PVA—DMSO solutions.[25]

On ageing of the Chl *a*–NC–DMSO solution (in a time-range of days) complex changes in spectral properties are

Table 1. Absorption parameters of Chl *a* in solutions, NC and PVA film

Chl *a* in	Concentration of solution (*M*); film (mol/g)	λ, Soret maximum (nm)	λ, Q_Y maximum (nm)	ϵ_S (M^{-1} cm^{-1})	S/Q_Y	FWHM Q_Y-band (cm^{-1})
DMSO	10^{-6}	432	665	95 000	1.28	500
NC-DMSO	10^{-6}	437	668	86 000	1.21	500
	10^{-5}	437	668	86 000	1.23	500
NC (low ratio)	10^{-7}	437	668	73 000	1.20	510
	9×10^{-6}	437	668	73 000	1.24	520
	10^{-5}	437	670/695	73 000	1.41	620
NC (high ratio)	5×10^{-7}	437	673/704	—	2.10	1570
	10^{-7}	434	668	90 000	1.25	520
PVA	5×10^{-7}	434	668/695	90 000	1.45	990
	5×10^{-6}	440	695/668	90 000	1.09	—

*The estimated error in the FWHM is 20 cm^{-1}. The estimated error in the extinction coefficient in the Soert maximum ϵ_S is 5000 M^{-1} cm^{-1}.

Table 2. Fluorescence parameters of Chl *a* in solutions, NC and PVA film*

Chl *a* in	Concentration of solution (*M*); film (mol/g)	λ_{exc} (nm)	$\lambda_{max,em}$ (nm)	FWHM (cm^{-1})	Remarks
DMSO	10^{-6}	434	674	510	—
NC DMSO	10^{-6}	437	678	520	—
	10^{-5}	437	678	520	—
NC film	10^{-7}	437	674	530	Less than 0.5 g
	9×10^{-6}	437	674	530	per 5 mL
	10^{-5}	437	674	530	
NC film	5×10^{-7}	437	674	530	1 g per 5 mL
	5×10^{-7}	480	678/720	550	1 g per 5 mL
	5×10^{-7}	437	674	530	2 g per 5 mL
	5×10^{-7}	480	678/720	—	2 g per 5 mL
PVA film	10^{-7}	434	674	510	—
	5×10^{-7}	434	674	510	—
	5×10^{-6}	434	674	520	—

*The error in the FWHM is estimated to be 20 cm^{-1}.

observed. This will be the subject of future studies and will not be discussed here.

The observation that the spectral behavior of Chl *a* in NC–DMSO solutions does not exhibit any dependence on the NC/DMSO ratio does not by itself imply that a similar behavior will also be found in the films. Indeed, we have found that the spectral properties of Chl *a* in films cast from NC–DMSO solutions depend on the NC/DMSO ratios. Two regions can be distinguished, above and below a ratio of about 0.5 g NC per 5 mL DMSO.

Chl a in NC films cast from NC–DMSO solutions with less than 0.5 g NC/5 mL DMSO. The absorption spectra of Chl *a* in NC films in the concentration range 10^{-7} mol/g to 9×10^{-6} mol/g and for a concentration of 10^{-5} mol/g are shown in Fig. 4. The latter concentration appears to be the solubility limit of Chl *a* in NC. The corresponding spectral parameters are presented in Table 1. All the spectra exhibited a small red shift of 6 nm relative to DMSO solution spectra.

The Chl *a* absorption spectra for concentrations below 10^{-5} mol/g are characteristic of monomeric Chl *a*, while at 10^{-5} mol/g an extra peak at 694–696 nm is found. Moreover, the ratio S/Q_Y and the FWHM of the Q_Y-band are also higher at this latter concentration. A similar behavior was found for PVA films (see above) only at much lower Chl *a* concentration.

The emission spectrum of Chl *a* in the films is identical to the monomeric spectrum and furthermore is found to be independent of the excitation wavelength and the concentration (Fig. 2). The corresponding spectral parameters are shown in Table 2. Excitation at 694–696 nm did not give rise to fluorescence emission in the 700–800 nm region. Again, the excitation spectra are found to be independent of the emission wavelength observed and correspond to the monomeric absorption spectra. We thus conclude that the species absorbing at 694–696 nm does not fluoresce.

The fluorescence intensity decay of Chl *a* in these films is found to be independent of the excitation and emission

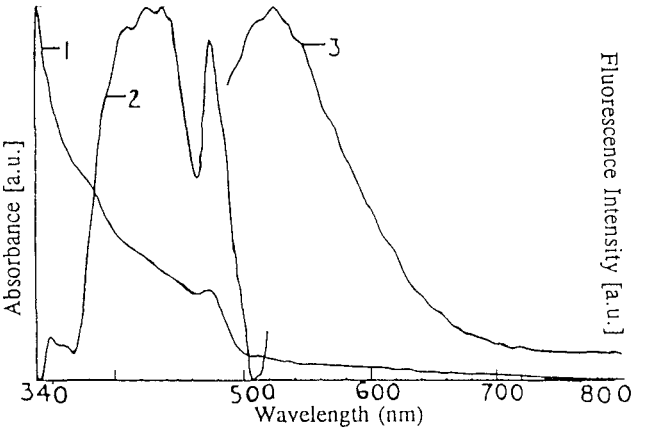

Figure 3. (1) Absorption spectrum of pure NC film; (2) excitation spectrum of pure NC film for emission at 540 nm; (3) emission spectrum of a pure NC film for excitation at 480 nm.

wavelength. On the other hand, the decay behavior changes from monoexponential for Chl *a* concentrations up to 10^{-6} mol/g to biexponential at higher concentrations. Interestingly, the changeover occurs before the appearance of the 694–696 absorption peak. The lifetime in the monoexponential regime is 4.4–4.7 ns but shortens considerably as a function of concentration in the biexponential range to an average value of 2.0–2.4 ns at 10^{-5} mol/g (Table 3). This indicates that at concentrations above 10^{-6} mol/g self-quenching becomes important.

Finally, fluorescence anisotropy measurements also reveal distinct behavior for different Chl *a* concentrations. At low concentrations, below 3×10^{-7} mol/g, the anisotropy is constant on the timescale of the fluorescence lifetime. We thus conclude that rotational motion of the Chl *a* molecules is quenched and that no ET takes place. The values of r(0) found (Table 4) are in good agreement with literature values.[25,56–58] At higher concentrations, the fluorescence anisotropy decays, presumably as a result of the ET processes.

Chl a in NC films cast from NC–DMSO solution with more than 0.5 g NC/5 mL DMSO. The absorption spectra for two films prepared from NC–DMSO solutions containing 0.5 g and 2 g NC in 5 mL DMSO, respectively, are shown in Fig. 5. The corresponding parameters are summarized in Table 1. The concentration of Chl *a* in both films is 5×10^{-7} mol/g NC. It is clear that an additional absorption peak around 705 nm arises on increasing the NC/DMSO ratio in the solution from which the films are cast. The appearance of this peak is accompanied by a broadening of the Soret band.

In contrast with our findings in PVA films and NC films cast from solutions with a low NC/DMSO ratio, the additional absorption peak now gives rise to a weak fluorescence band at 720 nm. This is concluded from the excitation spectra of the film cast from a solution containing 2 g NC in 5 mL DMSO (Fig. 6). For observation at 680 nm the excitation spectrum corresponds to the monomeric spectrum. On the other hand the excitation spectrum observed at 720 nm exhibits two additional peaks at 480 nm and around 705 nm. Furthermore the Soret band is significantly broadened as is also the case for the absorption spectrum.

The emission spectrum and its parameters for excitation

Table 3. Results of lifetime experiments*

Chl *a* in	Concentration of solution (*M*); film (mol/g)	λ_{ex} (nm)	λ_{em} (nm)	A_1 (%)	A_2 (%)	T_1 (ns)	T_2 (ns)
DMSO	10^{-6}	620	680	100	—	5.4	—
NC–DMSO	10^{-6}	660	680	100	—	4.7	—
NC film	10^{-7}	660	680	100	—	4.6	—
	3×10^{-7}	660	680	100	—	4.6	—
	5×10^{-7}	660	680	100	—	4.6	—
	10^{-6}	660	680	80	20	4.7	1.3
	5×10^{-6}	660	680	60	40	3.1	1.3
	10^{-5}	660	680	70	30	2.7	1.0
NC film (2 g on 5 mL)	3×10^{-7}	437	680	100	—	4.6	—
	3×10^{-7}	437	720	78	22	4.5	1.0
	3×10^{-7}	480	720	54	46	4.5	1.2

*Decay curves fit to $F(t) = A_1 \times e^{-t/T_1} + A_2 \times e^{-t/T_2}$. The estimated error in the lifetimes is 0.2 ns.

at 430 nm and 480 nm are shown in Fig. 7 and Table 2, respectively, for the film cast from an NC/DMSO solution containing 2 g NC per 5 mL DMSO. For excitation at 480 nm the emission spectrum of the latter shows significant deviations from the typically monomeric emission spectrum obtained by excitation at 430 nm. In particular, a broad structureless band at 510–540 nm, typical for fluorescence from NC chains (see Fig. 3) is observed in addition to a band at 720–730 nm.

We thus believe that the excitation peak at 480 nm arises from absorption by the NC chains. This peak is absent in the absorption spectrum since the latter has been corrected for the absorption of the polymer. However, because the pure NC matrix only exhibits fluorescence emission in the 510–540 nm region and not around 720 nm (see Fig. 3), the fluorescence in the latter region on excitation of the NC chains can only arise from interaction of these chains with Chl *a* pigments, *e.g. via* a complex.

The fluorescence intensity decay of Chl *a* in the films was measured in order to further characterize the nature of the species absorbing at 480 nm and 705 nm. A monoexponential decay behavior is observed for the emission band at 680 nm with a fluorescence lifetime of 4.4–4.7 ns independent of the excitation wavelength. In contrast, the fluorescence decay behavior for the emission band at 720 nm is best described by a biexponential function and is moreover dependent on the excitation wavelength. On excitation at 437 nm the major decay component has a lifetime of 4.5 ns, and the minor component of 1 ns (Table 3). The decay behavior on excitation at 480 ns is characterized by two components of equal weights and with the same lifetimes as found for excitation at 437 nm.

Finally, we note that the density of the NC films increased substantially with the NC/DMSO ratio in the solution from which they are cast (Table 5). This observation has a bearing on the formation of the fluorescing Chl *a* complex at 720 nm as will be discussed below.

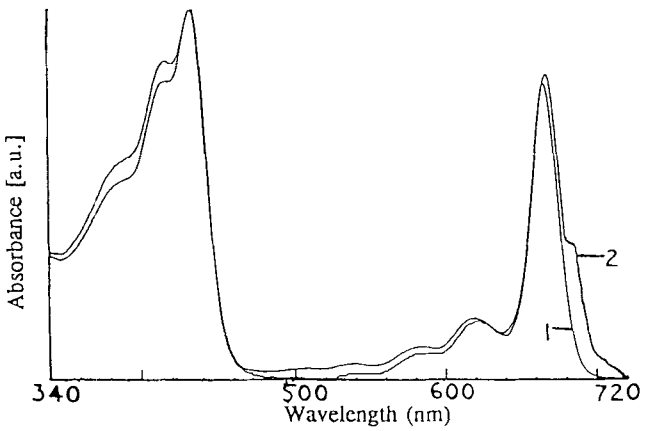

Figure 4. Absorption spectra of (1) Chl *a* in NC film prepared from solution with low NC to DMSO ratio, 5×10^{-7} mol/g; (2) Chl *a* in NC film prepared from solution with low NC to DMSO ratio, 10^{-5} mol/g.

ET study of Chl a in NC films cast from solutions with 0.3 g NC per 5 mL DMSO

The natural lifetime of Chl a in NC films. Since the natural lifetime of Chl *a* is expected to be influenced by the surrounding medium,[59] we have determined it in the NC films from the measured extinction and emission spectrum using Eq. 4. The value of 9.4 ± 1.0 ns found is subject to a relatively big error mainly caused by the error in the determination of the density of NC films. This value is significantly smaller than those reported for Chl *a* in various organic solvents, 11–15 ns. Interestingly, this implies that the quantum yield of Chl *a* in NC films is higher than that in these solvents, since the fluorescence lifetime is virtually un-

Table 4. Fluorescence anisotropy measurements ($r(t) = r(0)e^{-t/Tc}$) using synchrotron radiation as a light source*

Chl *a* in	Concentration (mol/g)	λ_{ex} (nm)	r(0)	T_c (ns)
NC film	10^{-7}	395	0.17	++
	3×10^{-7}	380	0.21	++
	3×10^{-7}	660	0.33	++

*The estimated error in r(0) is 0.02; emission wavelength is 680 nm; ++ means that no decay of anisotropy was observed within the fluorescence lifetime.

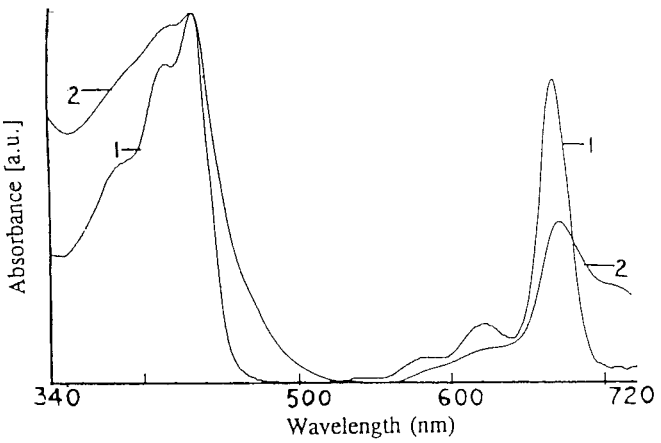

Figure 5. Absorption spectra of (1) Chl *a* in NC film prepared from solution with low NC to DMSO ratio, 5×10^{-7} mol/g; (2) Chl *a* in NC film prepared from solution with high NC to DMSO ratio, 5×10^{-7} mol/g.

affected by the medium. This could be explained by the absence of motions and collisions in the rigid NC medium.

Spectral determination of the Förster radius. The Förster radius, R_0, of Chl *a* in NC films obtained using Eq. 8 was found to be 59 ± 5 Å. Again, the error arises mainly from the uncertainties in the determination of the film density. This value is in good agreement with those found previously in organic solvents (for references see Knox[34]).

Determination of the Förster radius from fluorescence anisotropy decays. The fluorescence anisotropy decay curves were acquired as a function of Chl *a* concentration in unstretched NC films. The reduced Chl *a* concentration was calculated from Eq. 6, assuming a uniform pigment distribution. The decay behavior was well described by $r(t) = r(0)e^{-\sqrt{t/T_c}}$ with values of χ^2 between 1.0 and 1.2 over the entire concentration range studied. The values of T_c listed in Table 6 were found to be independent of the excitation and emission wavelengths. The fluorescence lifetimes and the values of r(0) extracted from the analysis were in excellent agreement with those reported by us in Table 4. Importantly,

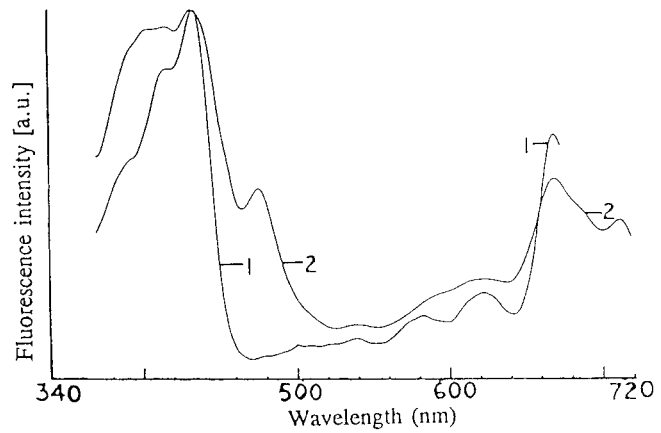

Figure 6. Excitation spectra of (1) Chl *a* in NC film from solution with 2 g NC on 5 mL DMSO, 5×10^{-7} mol/g, emission at 680 nm; (2) Chl *a* in NC films from solution with 2 NC on 5 mL DMSO, 5×10^{-7} mol/g, emission at 720 nm.

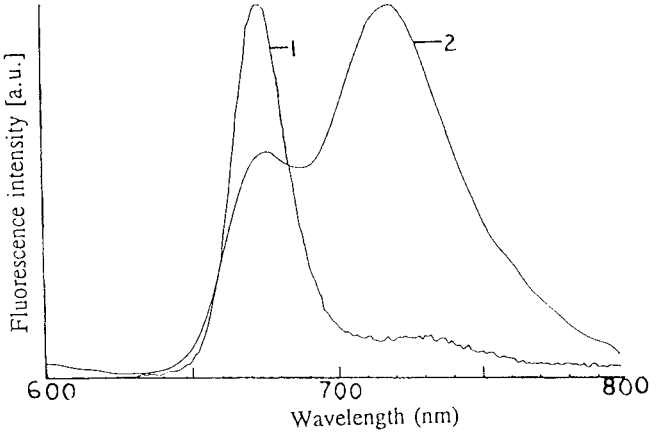

Figure 7. Emission spectra of Chl *a* in NC film from solution with 2 g NC on 5 mL DMSO, 5×10^{-7} mol/g; (1) excitation at 430 nm; (2) excitation at 480 nm.

the fluorescence anisotropy decays to zero at long times in agreement with the predictions of the Galanin approximation.

The results (Table 6) show that in the concentration range between 3×10^{-7} mol/g and 10^{-6} mol/g the decay time T_c is inversely proportional to the square of the reduced concentration in agreement with Eq. 5. A Förster radius R_0 of 61 ± 2 Å is now obtained from Eq. 5 and 6. This behavior, however, breaks down for concentrations above 10^{-6} mol/g.

DISCUSSION

We have previously shown that Chl *a* is present in a monomeric form in PVA films at concentrations below 4×10^{-7} mol/g.[25] The pigments are immobilized on the timescale of the fluorescence lifetime and are organized in a pocket-like structure. An efficient intermolecular ET mechanism operates in these pockets, but energy trapping by statistical pairs takes place. We have shown above that a nonfluorescing Chl *a* aggregate is formed on increasing the Chl *a* concentration up to 5×10^{-6} mol/g.

The question now arises as to the nature of this aggregate. A large variety of aggregates and complexes of Chl *a* molecules are known to exist and have been studied extensively in different media.[9-12,60-69] Of these only two aggregates resemble those found here in anhydrous PVA films. The first is a Chl *a*–H_2O–Chl *a* aggregate found in mixtures of inorganic and organic solvents, water–methanol mixtures and in aqueous PVA films. The maximum of the absorption band

Table 5. Density and thickness of NC films prepared using different NC to DMSO ratios in the original solutions*

Amount NC (g)	Amount DMSO (mL)	Thickness (μm)	Density (g/mL)
0.300	5.00	30	0.7
0.500	5.00	50	1.1
1.000	5.00	100	1.4
2.000	5.00	200	1.7

*Error in NC amount 0.002 g; error in DMSO amount 0.01 mL; error in thickness and density 10%.

Table 6. Results of fluorescence anisotropy decay measurements on unstretched Chl *a*–NC films*

c (mol/g)	ρ (molecules/m^3)	T_c (ns)
3.4×10^{-7}	1.4×10^{23}	372
5.7×10^{-7}	2.4×10^{23}	151
1.1×10^{-6}	4.6×10^{23}	42
5.6×10^{-6}	2.3×10^{24}	2
9.7×10^{-6}	3.5×10^{24}	4

*The error in the decay times is 5%.

depends on the medium but is generally centered around 700 nm. However, this aggregate exhibits a fluorescence band that is absent in our case. A second argument against the identification of this aggregate with the species reported above is the anhydrous conditions under which the PVA films were prepared, although we are aware of the fact that only traces of water could lead to aggregates of Chl *a* with water.[2,3] The second aggregate is found in some H_2O–DMSO mixtures and has been attributed to a linear [Chl *a*–DMSO]$_n$ polymer.[63] The formation of this aggregate was ascribed to the linear organization of DMSO in H_2O in certain mixtures. We believe that the aggregate reported here in anhydrous PVA films has a similar structure. This aggregate is most likely formed in the final stages of the film preparation procedure. Our findings thus suggest that the presence of water is not essential for its formation. We would like to stress, however, that the structure of the aggregate cannot be determined from fluorescence experiments alone. Further investigations of the structure are currently in progress.

The observations presented above underscore our previous contention that the Chl *a*–anhydrous PVA system is a suitable model system for the study of intermolecular ET processes in the presence of a high concentration of traps. However, the Chl *a* concentration in the PVA film must not exceed 4×10^{-7} mol/g. In a following paper we will study the influence of uniaxial stretching of the films on the distribution and state of Chl *a*.

The results on the NC systems presented above clearly demonstrate that Chl *a* exists in a pure monomeric state in NC–DMSO solution under all the experimental conditions used. In contrast, the state of the pigments in NC films cast from these solutions depends strongly on the NC/DMSO ratio. A fluorescing Chl *a* complex is present in films prepared from solutions containing more than 0.5 g NC in 5 mL DMSO. We believe that this is a Chl *a*–NC complex for the following reasons. (1) Excitation of a pure NC film at 480 nm gives rise to a broad emission band around 540 nm, while a Chl *a*/NC film exhibits emission bands around 540 nm and 720 nm at the same excitation wavelength. (2) The excitation spectrum of the Chl *a*/NC films monitored at 720 nm has peaks at 480 nm and 705 nm. The latter peak is also present in the absorption spectrum. The 480 nm peak has effectively been removed from the film absorption spectrum due to the correction for absorption by the NC matrix.

We thus conclude that a fluorescing Chl *a*–NC complex is present in the films. The fluorescence emission can be excited by illuminating the film either at 705 nm or at 480 nm, the absorption peak of the NC chains. The formation of this complex, in which efficient ET between the Chl *a* pigments and the NC chains takes place, requires a close packing in the film. Indeed, pure NC films formed from solutions with a high NC/DMSO ratio are found to have a substantially higher density than those formed from solutions with a low NC/DMSO ratio (Table 5). Further characterization of the Chl *a*–NC complex is beyond the scope of this paper but is currently in progress.

The interaction between Chl *a* molecules in NC films prepared from solutions containing less than 0.5 g NC in 5 mL DMSO can be modulated simply by changing the concentration of the pigments. Aggregates are only formed at concentrations close to the solubility limit of Chl *a* in NC, 10^{-5} mol/g. This aggregate exhibits the same characteristic spectral properties as the one reported above in anhydrous PVA films. Nitrocellulose films containing smaller Chl *a* concentrations exhibit spectral properties characteristic of the monomeric state. At Chl *a* concentrations less than 3×10^{-7} mol/g, the fluorescence intensity decay is monoexponential with a lifetime of 4.4–4.7 ns. Moreover, the fluorescence anisotropy is constant on this timescale. The value of the anisotropy is in good agreement with literature values for monomeric Chl *a*. We can thus conclude that the pigments are separated by large distances so that no ET can take place. On decreasing the distances between the Chl *a* molecules, intermolecular ET processes are induced. This happens in the concentration range of 3×10^{-7} mol/g to 10^{-6} mol/g, where the fluorescence anisotropy decays while the intensity decay maintains its monoexponential behavior. On increasing the Chl *a* concentration further up to the solubility limit, the fluorescence intensity decay exhibits a biexponential behavior with a shortened average lifetime. This indicates the formation of statistical traps in the NC matrix.

Finally, we want to establish whether the monomeric Chl *a* molecules in an NC film cast from 0.3 g NC per 5 mL DMSO are distributed uniformally within the matrix. To this end we have used a combination of steady-state spectral and time-resolved fluorescence anisotropy experiments to investigate the distribution of Chl *a* pigments in NC films. In particular we have focused on the agreement between the experimental observations and the predictions of donor–donor ET theory derived on the assumption of uniform and isotropic pigment distribution. The agreement is judged using two criteria. In the first place, the reduced concentration extracted from the fluorescence anisotropy decays should scale linearly with the overall average pigment concentration. Secondly, the Förster radius R_0 obtained from this relation should correspond with the value extracted from the spectral parameters. We have found that both criteria are met for NC films containing between 3×10^{-7} mol/g and 10^{-6} mol/g Chl *a*. Films with a lower Chl *a* concentration exhibited no ET as evidenced by a constant fluorescence anisotropy on the timescale of the fluorescence lifetime, while at concentrations above 10^{-6} mol/g we found a shortening of the fluorescence lifetime due to trapping by statistical pairs and thus according to Eq. 7 the anisotropy decay becomes much more complex.

We have therefore every reason to believe that Chl *a* pigments are uniformly distributed in the unstretched NC matrix at concentrations below 10^{-6} mol/g.

The results presented here show unambiguously that un-

stretched Chl *a*/NC films cast from solutions with less than 0.5 g NC per 5 mL DMSO can be particularly suitable model systems for studying intermolecular ET processes. The state and organization of Chl *a* in NC films after uniaxial stretching will be the subject of our next study, since investigation of the effect of the mutual orientation of the pigments on the process can only be carried out in uniaxially stretched films. The stretching of the film causes macroscopic and microscopic alignment of the Chl *a* molecules. Importantly, stretched films with a low Chl *a* concentration, where no ET processes take place, may be used in the determination of the directions of the transition dipole moments in the molecular frame of the pigments.

Acknowledgements—M.A.M.J.v.Z. was supported by the Dutch Foundation of Chemistry (SON) under the auspices of the Netherlands Organisation of Scientific Research (NWO). The use of the synchrotron radiation source was made possible by NWO by the agreement between SERC and NWO.

REFERENCES

1. Ort, D. R. and Govindjec (1987) Obschie predstavlenia o preobrazovanie energii pri fotosintezi (General review energy transformation in photosynthesis). In *Fotosintez*, Vol. 1 (Edited by Govindjee), pp. 8–89. Mir, Moskva.
2. Kelly, A. R. and G. Porter (1970) Model systems for photosynthesis. I. Energy transfer and light harvesting mechanisms. *Proc. R. Soc. London A* **315**, 149–161.
3. Kelly, A. R. and G. Porter (1971) Model systems for photosynthesis. II. Concentration quenching of chlorophyll b fluorescence in solid solutions. *Proc. R. Soc. Lond. A* **324**, 117–126.
4. Beddard, G. S. and G. Porter (1976) Concentration quenching in chlorophyll. *Nature* **260**, 366–367.
5. Dalton, J. (1980) Concentration quenching in chlorophyll. *J. Chem. Soc. Chem. Commun.* **3**, 78–80.
6. Wong, D., K. Vacek, H. Merkelo and Govindjee (1978) Excitation energy transfer among chlorophyll a molecules on polystyrene: concentration dependence of quantum yield, polarization and lifetime of fluorescence. *Z. Naturforsch.* **33c**, 863–869.
7. Boulu, L. G., L. K. Patterson, J. P. Chauvet and J. J. Kozak (1986) Theoretical investigations of fluorescence concentration quenching in two-dimensional disordered systems. Application to chlorophyll *a* in monolayers of dioleoylphosphatidylcholine. *J. Chem. Phys.* **86**, 503–507.
8. Tweet, A. G., W. D. Bellamy and G. L. Gaines, Jr. (1964) Fluorescence quenching and energy transfer in monomolecular films containing chlorophyll. *J. Chem. Phys.* **41**, 2068–2077.
9. Inamura, I., H. Ochiai, K. Toki, S. Watanabe, S. Hikino and T. Araki (1983) Preparation and properties of chlorophyll/water soluble macromolecular complexes in water. Stabilization of chlorophyll aggregates in the water-soluble macromolecule. *Photochem. Photobiol.* **38**, 37–44.
10. Inamura, I. (1987) Solubilization of chlorophyll *a*–dioxane complex in water by polyvinyl alcohol. *Chem. Lett.* **1980**, 1607–1610.
11. Uehara, K., M. Mimuro, Y. Fujita and M. Tanaka (1988) Spectral analysis of chlorophyll *a* aggregates in the presence of water-soluble macromolecules. *Photochem. Photobiol.* **48**, 725–732.
12. Seely, G. R. (1992) On the origin of 628 nm fluorescence in certain chlorophyll preparations. *Photochem. Photobiol.* **55**, 319–322.
13. Förster, Th. (1948) Zwischenmolekulare Energiewanderungen und Fluorescenz. *Ann. Phys.* **2**, 55–73.
14. Bonart, R. (1969) Kristall- und Kolloidstrukturen beim Dehnen und Verstrecken. *Kolloid Z.* **231**, 438–458.
15. Xixiong, Z. (1993) Analysis of mechanical behaviour in cold-drawing deformation of polymers. *J. Polym. Sci. B Polym. Phys.* **31**, 1667–1675.
16. Sawatari, C., Y. Yamamoto, N. Yanagida and M. Matsuo (1992) Drawability of poly(vinyl alcohol) films prepared by gelation/crystallization from semidilute solutions. *Polymer* **34**, 956–966.
17. Nashijima, Y., Y. Onogi, R. Yamazaki and K. Kawakami (1968) Molecular orientation behaviour in polyvinylalcohol films studied by the fluorescence method. (I) Uniaxial deformations. *Rep. Prog. Polym. Phys. Jpn.* **11**, 407–410.
18. Tanizaki, Y. (1959) Dichroism of dyes in the stretched PVA sheet. II. *J. Chem. Soc. Jpn. Pure Chem. Sec.* **78**, 75–80.
19. Spegt, P., B. Meurer, C. Hornick and G. Weill (1985) Molecular orientation in stretched poly(vinylalcohol). I. NMR anisotropy and birefringence. *J. Polym. Sci. Polym. Phys. Ed.* **23**, 315–325.
20. Ward, M. (1977) The measurement of molecular orientation in polymers by spectroscopic techniques. *J. Polym. Sci. Polym. Symp.* **58**, 1–21.
21. Swalen, J. D., M. Tacke, R. Santo and J. Fisher (1976) Determination of optical constants of polymeric thin films by integrated optical techniques. *Optical Commun.* **18**, 387–390.
22. Van Gurp, M. and Y. K. Levine (1988) Determination of transition moment directions in molecules of low symmetry using polarized fluorescence. I. Theory. *J. Chem. Phys.* **90**(8), 4095–4102.
23. Van Gurp, M. and Y. K. Levine (1988) Determination of transition moment directions in molecules of low symmetry using polarized fluorescence. II. Application to pyranine, perylene and DPH. *J. Chem. Phys.* **90**(8), 4103–4111.
24. Van der Heide, U. A., B. Orbons, H. C. Gerritsen and Y. K. Levine (1992) The orientation of transition moments of dye molecules used in fluorescence studies of muscle systems. *Eur. Biophys. J.* **21**, 263–272.
25. Van Zandvoort, M. A. M. J., D. Wróbel, A. J. Scholten, D. de Jager, G. van Ginkel and Y. K. Levine (1993) Spectroscopic study of chlorophyll *a* in organic solvents and polymerized anhydrous polyvinyl matrix. *Photochem. Photobiol.* **58**, 600–606.
26. Förster, Th. (1960) Transfer mechanisms of electronic excitation energy. *Radiat. Res. Suppl.* **2**, 326–339.
27. Förster, Th. (1967) Mechanisms of energy transfer. *Comp. Biochem.* **22**, 61–78.
28. Haan, S. W. and R. Zwanzig (1977) Förster migration of electronic excitation between randomly distributed molecules. *J. Chem. Phys.* **68**, 1879–1883.
29. Baumann, J. and M. D. Fayer (1986) Excitation transfer in disordered two-dimensional and anisotropic three-dimensional systems: effects of spatial geometry on time-resolved observables. *J. Chem. Phys.* **85**, 4087–4107.
30. Knoester, J. and J. E. van Himbergen (1984) Excitation decay due to incoherent energy transfer: a comparative study of means of an exact density expansion. *J. Chem. Phys.* **80**, 4200–4203.
31. Knoester, J. and J. E. van Himbergen (1984) Effect of molecular reorientation on excitation decay due to incoherent energy transfer. *J. Chem. Phys.* **81**, 4380–4388.
32. Knoester, J. and J. E. van Himbergen (1986) Theory of concentration depolarization in the presence of orientational correlations. *J. Chem. Phys.* **84**, 2990–2997.
33. Knoester, J. and J. E. van Himbergen (1987) On the theory of concentration selfquenching by statistical traps. *J. Chem. Phys.* **86**, 3571–3576.
34. Knox, R. S. (1975) Excitation energy transfer and migration: theoretical considerations. In *Bioenergetics in Photosynthesis* (Edited by Govindjee), pp. 183–222. Academic Press, New York.
35. Knox, R. S. (1972) Transfer of electronic excitation energy in condensed systems. *Lectures for NATO Advanced Study Institute on Primary Molecular Events in Photobiology*, Florence, Italy.
36. Scholes, G. D., H. A. Clayton and K. P. Ghiggino (1992) On the rate of radiationless intermolecular energy transfer. *J. Chem. Phys.* **97**, 7405–7413.
37. Birks, J. B. (1970) *Photophysics of Aromatic Molecules*. Wiley-Interscience, London.
38. Hart, D. E., P. A. Anfinrud and W. S. Struve (1986) Excitation transport in solution: a quantitative comparison between GAF

theory and time-resolved fluorescence profiles. *J. Chem. Phys.* **86**, 2689–2696.
39. Huber, D. L., D. S. Hamilton and B. Barnett (1977) Time-dependent effects in fluorescent line narrowing. *Phys. Rev. B* **16**, 4642–4650.
40. Galanin, M. D. (1955) The problem of the effect of concentration on the luminescence of solutions. *Sov. Physics-JETP.* **1**(2), 317–325.
41. Terpstra, W. and W. J. Lambers (1983) Incorporation of chlorophyll *a* and chlorophyllase into artificial membranes. *Photobiochem. Photobiophys.* **6**, 93–100.
42. Roy, S. (1987) High performance liquid chromatographic analysis of chloropigments. *J. Chromatogr.* **391**, 19–34.
43. Hynninen, P. H. and N. Ellfolk (1973) Chlorophylls. I. Separation and isolation of chlorophylls a and b by multiple liquid–liquid partition. *Acta Chem. Scand.* **27**, 1463–1477.
44. Hynninen, P. H. and S. Assandri (1973) Chlorophylls. II. Allomerization of chlorophylls a and b. *Acta Chem. Scand.* **27**, 1478–1486.
45. Hynninen, P. H. (1973) Chlorophylls. III. Keto–enol tautomerism of chlorophylls a and b. The nature of chlorophylls a′ and b′. *Acta Chem. Scand.* **27**, 1487–1495.
46. Hynninen, P. H. (1973) Chlorophylls. IV. Preparation and purification of some derivatives of chlorophylls a and b. *Acta Chem. Scand.* **27**, 1771–1780.
47. Hynninen, P. H. (1977) Chlorophylls. V. Isolation of chlorophylls a and b using an improved two-phase extraction method followed by a precipation and a separation on a sucrose column. *Acta Chem. Scand.* **31**, 829–835.
48. Hynninen, P. H., M. R. Wasielewski and J. J. Katz (1979) Chlorophylls. VI. Epimerization and enolization of chlorophyll a and its magnesium-free derivatives. *Acta Chem. Scand.* **33**, 637–648.
49. Scholz, B. and K. Ballschmiter (1981) Preparation and reversed-phase high-performance liquid chromatography of chlorophylls. *J. Chromatogr.* **208**, 148–155.
50. Watanabe, T., H. Mazaki and M. Nakazato (1987) Chlorophyll a/a′ epimerization in organic solvents. *Biochim. Biophys. Acta* **892**, 197–206.
51. Munro, I. H. and N. Schwentner (1983) Time resolved spectroscopy using synchrotron radiation. Nucl. Instrum. Methods **208**, 819–834.
52. Van Langen, H., Y. K. Levine, M. Ameloot and H. Pottel (1987) Ambiguities in the interpretation of time-resolved fluorescence anisotropy measurements on lipid vesicle systems. *Chem. Phys. Lett.* **140**, 394–400.
53. Zannoni, C. (1980) A theory of fluorescence depolarization in membranes. *Mol. Phys.* **42**, 1303–1320.
54. Connolly, J. S., A. F. Janzen and E. B. Samuel (1982) Fluorescence lifetimes of chlorophyll a: solvent, concentration and oxygen dependence. *Photochem. Photobiol.* **36**, 559–563.
55. Cotton, T. M., P. A. Loach, J. J. Katz and K. Ballschmitter (1978) Studies of chlorophyll–chlorophyll and chlorophyll–ligand interactions by visible absorption and infrared spectroscopy at low temperatures. *Photochem. Photobiol.* **27**, 735–749.
56. Van Gurp, M., G. van Ginkel and Y. K. Levine (1988) Fluorescence anisotropy of chlorophyll *a* and chlorophyll *b* in caster oil. *Biochim. Biophys. Acta* **973**, 405–413.
57. Kuki, A. and S. G. Boxer (1983) Chlorophyllide substituted hemoglobin tetramers and hybrids: preparation, characterization and energy transfer. *Biochemistry* **22**, 2923–2925.
58. Kwa, S. L. S., S. Völker, N. T. Tilly, R. Van Grondelle and J. P. Dekker (1993) Polarized site-selection spectroscopy of chlorophyll *a* in detergent. *Photochem. Photobiol.* **59**(2), 219–228.
59. Fetisova, Z. G. and A. Yu. Borisov (1973) The intrinsic lifetimes of bacterioviridin-660 and chlorophyll in different solvents. *J. Photochem.* **2**, 51–59.
60. Ballschmitter, K., T. M. Cotton, H. H. Strain and J. J. Katz (1969) Chlorophyll-water interaction hydration, dehydration and hydrates of chlorophyll. *Biochim. Biophys. Acta* **180**, 347–359.
61. Fong, F. K. and V. J. Koester (1976) *In vitro* preparation and characterization of a 700 nm absorbing chlorophyll–water adduct according to the proposed primary molecular unit in photosynthesis. *Biochim. Biophys. Acta* **423**, 52–64.
62. Katz, J. J., L. L. Shipman, T. M. Cotton and T. R. Janson (1978) Chlorophyll aggregation: coordination interactions in chlorophyll monomers, dimers and oligomers. In *The Porphyrins.* Vol. 5, part C (Edited by D. Dolphin), pp. 401–458. Academic Press, New York.
63. Uehara, K., M. Mimuro and M. Tanaka (1991) Spectroscopic studies of chlorophyll *a* aggregates formed by aqueous dimethyl sulfoxide. *Photochem. Photobiol.* **53**, 371–377.
64. Helenius, V., J. Erostyàk and J. Korppi-Tommola (1991) Aggregation of chlorophyll *a* in hydrocarbon solution. *Inst. Phys. Conf. Ser.* **126**(VIII), 623–626.
65. Helenius, V. M., P. H. Hynninen and J. E. I. Korppi-Tommola (1993) Chlorophyll *a* aggregates in hydrocarbon solution, a picosecond spectroscopy and molecular modeling study. *Photochem. Photobiol.* **58**, 867–873.
66. Fragata, M. (1977) A far-red absorbing form of chlorophyll *a* detected in phosphatidylcholine vesicles. *Photosynthetica* **11**, 296–301.
67. Frąckowiak, D., D. Bauman, H. Manikowski and T. Martyński (1977) Spectral properties of chlorophyll *a* in liquid crystal. *Biophys. Chem.* **6**, 369–377.
68. Frąckowiak, D., J. Szurkowski, B. Szych, S. Hotchandani and R. M. Leblanc (1985) Spectra of chlorophyll *a* and *b* and their aggregates in nematic liquid crystals and polyvinyl alcohol films. *Photobiochem. Photobiophys.* **12**, 9–19.
69. Frąckowiak, D. and R. M. Leblanc (1994) Fluorescence of aggregated forms of chlorophyll *a* in various media. *J. Photochem. Photobiol. A Chem.* **78**, 49–55.